HHS Public Access

Author manuscript

Cell Host Microbe. Author manuscript; available in PMC 2020 November 13.

Published in final edited form as:

Cell Host Microbe. 2019 November 13; 26(5): 591–600.e4. doi:10.1016/j.chom.2019.10.001.

Adenovirus Vector-Based Vaccines Confer Maternal-Fetal Protection Against Zika Virus Challenge in Pregnant IFNαR$^{-/-}$ Mice

Rafael A. Larocca[1], **Erica A. Mendes**[1,2], **Peter Abbink**[1], **Rebecca L. Peterson**[1], **Amanda J. Martinot**[1], **M. Justin Iampietro**[1], **Zi H. Kang**[1], **Malika Aid**[1], **Marinela Kirilova**[1], **Catherine Jacob-Dolan**[1], **Lisa Tostanoski**[1], **Erica N. Borducchi**[1], **Rafael A. De La Barrera**[3], **Dan H. Barouch**[1,4,5,*]

[1]Center for Virology and Vaccine Research, Beth Israel Deaconess Medical Center, Harvard Medical School, Boston, MA 02215, USA

[2]University of São Paulo, São Paulo, SP 05508-000, Brazil

[3]Walter Reed Army Institute of Research, Silver Spring, MD 20910, USA

[4]Ragon Institute of MGH, MIT and Harvard, Cambridge, MA 02139, USA

[5]Lead Contact

SUMMARY

Maternal infection with Zika virus (ZIKV) can lead to microcephaly and other congenital abnormalities of the fetus. Although ZIKV vaccines that prevent or reduce viremia in non-pregnant mice have been described, a maternal vaccine that provides complete fetal protection would be desirable. Here we show that adenovirus (Ad) vector-based ZIKV vaccines induce potent neutralizing antibodies that confer robust maternal and fetal protection against ZIKV challenge in pregnant, highly susceptible IFN-αβR$^{-/-}$ mice. Moreover, passive transfer of maternal antibodies from vaccinated dams protected pups against postnatal ZIKV challenge. These data suggest that Ad-based ZIKV vaccines may be able to provide protection in pregnant females against fetal ZIKV transmission in utero as well as in infants against ZIKV infection after birth.

INTRODUCTION

Zika virus (ZIKV) is a mosquito-transmitted flavivirus, which includes dengue virus, yellow fever virus, West Nile virus, Japanese encephalitis virus, and tick-borne encephalitis virus (Richner and Diamond, 2018). In healthy adults, clinical ZIKV infection is typically mild,

*Correspondence: dbarouch@bidmc.harvard.edu (D.H.B).

AUTHOR CONTRIBUTIONS

R.A.L. and D.H.B. designed the studies. R.A.L. and E.A.M led animal work. P.A., R.L.P., and M.K. led the virologic assays. A.J.M. led the histopathologic analyses. R.A.D. performed neutralization studies. R.A.L., E.A.M., M.J.I., Z.H.K., M.A., C.J.D., L.H.T., and E.N.B led the specimen processing and sample analysis. R.A.L and D.H.B. wrote the paper with all co-authors.

DECLARATION OF INTERESTS

The authors declare no competing financial interests. R.A.L., P.A., and D.H.B. are co-inventors on a ZIKV antigen patent that has been licensed.

but in rare cases it can lead to Guillain Barré syndrome (Krauer et al., 2017). ZIKV infection during pregnancy can result in devastating consequences such as congenital Zika syndrome, with microcephaly in approximately 2–4 % of cases of ZIKV-infected pregnant woman and multiple other congenital abnormalities (Brasil et al., 2016; Satterfield-Nash et al., 2017). The development of a ZIKV vaccine that can protect fetuses in utero is therefore critical.

We and others have reported the protective efficacy of multiple ZIKV vaccine candidates in non-pregnant mice and monkeys (Abbink et al., 2016; Larocca et al., 2016; Shan et al., 2017). However, pregnant women infected with ZIKV demonstrate prolonged viremia (Suy et al., 2016), and thus vaccine protection in pregnant women may be more difficult than in non-pregnant individuals. Moreover, the goal of a ZIKV vaccine is to protect pregnant women and their fetuses against ZIKV infection. A recent report has shown that a live attenuated virus vaccine and an RNA vaccine for ZIKV resulted in partial efficacy in wildtype mice treated with an anti-IFNα receptor antibody (Richner et al., 2017). These vaccines, however, did not completely protect pregnant mice, and ZIKV RNA was readily detected following challenge in multiple tissues from both dams and fetuses. We previously demonstrated that Ad-based ZIKV vaccines were particularly potent and provided superior long-term protection than DNA vaccines and inactivated virus vaccines (Abbink et al., 2017). We therefore assessed whether Ad vector-based ZIKV vaccines could protect pregnant mice and their fetuses against ZIKV challenge.

Using the IFN-αβR$^{-/-}$ pregnancy model, unvaccinated dams challenged with ZIKV exhibited severe placental damage, resulting in intra-uterine growth restriction (IUGR) and fetal loss (Miner et al., 2016; Yockey et al., 2016). Here we show in a proof-of-concept study that a single immunization with an Ad26 or RhAd52 vector-based ZIKV vaccine afforded robust protection of IFN-αβR$^{-/-}$ dams and fetuses against ZIKV infection. Marginal or no ZIKV RNA was detected in placenta and fetal brain samples in vaccinated mice following ZIKV challenge. In addition, we demonstrate postnatal protection of pups born to vaccinated dams, presumably as a result of passive transfer of maternal antibodies.

RESULTS

RhAd52 and Ad26 ZIKV Vaccines Protect Non-Pregnant Mice Against ZIKV Challenge

We first sought to evaluate the protective efficacy of the RhAd52 vector-based vaccine expressing ZIKV M-Env in non-pregnant IFN-αβR$^{-/-}$ mice. We vaccinated a group of female IFN-αβR$^{-/-}$ mice (n = 4) by the intramuscular (IM) route with a single dose of 10^9 viral particles (vp) RhAd52.M-Env (Figure 1A). This vaccine regimen has previously been shown to protect both wildtype mice and monkeys against ZIKV challenge (Abbink et al., 2017; 2016). The RhAd52.M-Env vaccine elicited robust Env-specific binding and neutralizing antibody titers of 4.02 logs and 2.62 logs, respectively, as measured by ELISA and microneutralization (MN)-50 assays (p=0.02 comparing vaccinated and unvaccinated mice) (Figure 1B, 1C). To assess protective efficacy of this vaccine, we challenged these mice at week 4 by the intravenous (IV) route with 10^2 plaque forming units (PFU) of ZIKV-BR (Brazil/ZKV2015), which has previously been reported to cause IUGR in SJL mice and fetal neuropathology in rhesus monkeys (Cugola et al., 2016; Martinot et al., 2018). Unvaccinated sham IFN-αβR$^{-/-}$ mice inoculated with ZIKV-BR exhibited approximately 63

days of viremia with a mean peak viral load of 6.86 log copies / ml (range 6.42–7.65 copies / ml; n = 4) (Figure 1D). This prolonged viremia contrasts with shorter viremia of approximately 7 days in wildtype mice (Larocca et al., 2016). IFN-αβR$^{-/-}$ mice vaccinated with RhAd52.M-Env provided robust protection with undetectable serum viral RNA following ZIKV-BR challenge (Figure 1E).

We next vaccinated a group of female IFN-αβR$^{-/-}$ mice (n = 5) with a single dose of 10^9 vp of Ad26.M-Env (Abbink et al., 2017) (Figure S1A). Similar to RhAd52.M-Env, Ad26.M-Env elicited robust neutralizing antibody titers (mean MN50 titer 3.01 logs; p = 0.0079 comparing vaccinated with unvaccinated mice) (Figure S1B). At week 4 following vaccination, we challenged these mice with 10^2 PFU ZIKV-BR and assessed viral RNA in serum and in tissues on day 21 following challenge. Sham mice showed high levels of viral RNA in serum and tissues, whereas vaccinated mice demonstrated no detectable viral RNA in serum and marginal or no viral RNA in lymph nodes (LN), spleen, ovary, and brain following challenge (Figure S1C–S1H) ($p < 0.0079$ for all compartments compared with sham).

RhAd52 and Ad26 ZIKV Vaccines Protect Pregnant Mice Against ZIKV Challenge

We next assessed the immunogenicity and protective efficacy of RhAd52.M-Env and Ad26.M-Env against ZIKV-BR challenge in pregnant IFN-αβR$^{-/-}$ mice. Female IFN-αβR$^{-/-}$ mice were immunized IM with 10^9 vp RhAd52.M-Env (n = 9) or 10^9 vp Ad26.M-Env (n = 10). These vaccines induced robust Env-specific ELISA titers (mean 3.78–3.87 logs) (Figure 2B) and MN50 titers (mean 2.69–2.70 logs; p = 0.001 compared with controls) (Figure 2C). At week 4 after immunization, vaccinated female mice were mated with naïve wildtype C57BL/6 male mice. Pregnant mice were then challenged IV with 10^2 PFU ZIKV-BR on embryonic day (e)5.5 after observation of a vaginal plug. On day e17.5, we performed cesarean sections to obtain dam and fetal tissues for evaluation (Figure 2A). Maternal tissues from unvaccinated pregnant IFN-αβR$^{-/-}$ mice, including serum, spleen, LN, ovary, and brain, showed high levels of ZIKV RNA following challenge. In contrast, no ZIKV RNA was detected in serum or tissues from vaccinated pregnant mice following challenge (Figure 2D–2H) ($p < 0.0001$ for all compartments compared with sham).

RhAd52 and Ad26 ZIKV Vaccines Prevent Fetal Intrauterine Growth Restriction Following ZIKV Challenge

ZIKV has been reported to cause placental damage and fetal demise following infection of pregnant IFN-αβR$^{-/-}$ mice (Miner et al., 2016). To assess the impact of vaccination on fetal viability, individual fetuses were evaluated morphologically for body weight, length (crown-rump length; CRL), head length (occipital-frontal diameter; OF), and total body area (CRL × OF). Female IFN-αβR$^{-/-}$ mice were immunized with 10^9 vp of RhAd52.M-Env (n = 9) or 10^9 vp of Ad26.M-Env (n = 10) and challenged with 10^2 PFU of ZIKV-BR on embryonic days e5.5 following observation of vaginal plug, as in the previous experiment. Unvaccinated infected (sham) and uninfected (naïve) mice were included as positive and negative controls, respectively (Figure 3A). As expected, the majority (77.1%) of ZIKV-infected sham mice (64 of 83 pregnant sites (PS)) had fetal resorptions. In vaccinated mice, fetal resorption occurred at a much lower rate of 7.4% (RhAd52; 6 of 81 PS) and 8.54%

(Ad26; 7 of 82 PS), which was comparable to the 12.5% resorption rate observed in the uninfected naïve group (Naïve; 7 of 56 PS; Figure 3B). The rare viable fetuses from the infected sham group exhibited significant IUGR (Figure 3C, S2) with lower body weight than fetuses from vaccinated or uninfected naïve mice ($p < 0.0001$) (Figure 3D). Fetuses from the infected sham group also had reduced fetal length ($p < 0.0001$) (Figure 3E), head size ($p < 0.0001$) (Figure 3F), and body area (CRL × OF) ($p < 0.0001$) (Figure 3G). A partial least squares discriminant analysis (PLSDA) that compared all biometric parameters confirmed that the infected sham mice clustered separately from the vaccinated and uninfected naïve mice (Figure 3H).

RhAd52 and Ad26 ZIKV Vaccines Protect Placental and Fetal Tissues Following ZIKV Challenge

Previous reports have shown that certain vaccines can provide partial protection in pregnant mouse models (Prow et al., 2018; Richner et al., 2017; Wang et al., 2018). We therefore evaluated fetal and placental tissues from the RhAd52.M-Env and Ad26.M-Env vaccinated dams described above following ZIKV-BR challenge. All resorbed fetuses from the infected sham mice (n = 64) exhibited high levels of ZIKV RNA (mean 4.26 log copies / μg RNA; Figure 4A). In contrast, the few resorbed fetuses from the RhAd52 (n = 6) and Ad26 (n = 7) vaccinated animals showed no detectable ZIKV RNA (limit of detection (LOD) 1 copy / μg RNA; $p<0.0001$ comparing fetuses from vaccinated mice with sham mice) (Figure 4A). Moreover, placental tissues from infected sham mice (n = 28) had high levels of ZIKV RNA (mean 4.1 logs / μg RNA), whereas no ZIKV RNA was detected in placentas from RhAd52 (n = 75) and Ad26 (n = 75) vaccinated mice ($p < 0.0001$) (Figure 4B). In addition, 14 of 21 (66%) fetuses from infected sham mice demonstrated ZIKV RNA in their brains (mean 0.57 log / μg RNA), whereas no ZIKV RNA was detected in fetal brains from dams vaccinated with either RhAd52 (n = 75) or Ad26 (n = 75) ($p < 0.0001$; Figure 4C).

These results were confirmed by assessing placental tissues for the presence of ZIKV Env by immunohistochemistry. In infected sham mice, there was diffuse ZIKV Env staining in the fetal labyrinth and vascular spaces, but no ZIKV Env staining was detected in the placentas from RhAd52 or Ad26 vaccinated animals (Figure 5A). Moreover, ZIKV Env staining in the infected sham mice was observed in regions of high positivity for cytokeratin, consistent with infection of placental trophoblasts (Figure 5B).

Vaccine Protection Against High-Dose ZIKV Challenge

To evaluate the robustness of vaccine protection against a higher dose ZIKV-BR challenge, we immunized two groups of non-pregnant female IFN-$\alpha\beta R^{-/-}$ female mice with 10^9 vp of Ad26.M-Env (Figure S3A, S4A). Four weeks after immunization, the Ad26.M-Env vaccine elicited robust ZIKV-specific MN50 titers (Figure S3B, S4B), consistent with prior data. Vaccinated IFN-$\alpha\beta R^{-/-}$ female mice were mated with C57BL/6 male mice, and on day e5.5 after observation of a vaginal plug, pregnant mice were challenged IV with either 10^2 PFU or a higher dose of 10^3 PFU ZIKV-BR. On day e9.5, 4 days post challenge, maternal and fetal tissues were assessed for ZIKV RNA. Sham mice challenged with both 10^2 and 10^3 PFU ZIKV BR showed high levels of ZIKV RNA in serum, LN, spleen, ovary, and brain (Figure S3C–S3H, Figure S4C–S4H). Marginal or negative viral RNA was detected in

embryos of vaccinated mice challenged with 10^2 PFU (Figure S3C–S3H), whereas three embryos of vaccinated mice challenged with 10^3 PFU challenge showed low levels of viral RNA (Figure S4C–S4H). Taken together, 72 of 72 (100%) embryos from sham mice showed ZIKV RNA following challenge, whereas only 3 of 88 (3.4%) embryos from vaccinated mice showed detectable ZIKV RNA following challenge ($p<0.0001$) (Figures S3H, S4H).

Vaccine-Elicited Immune Responses Mediate Immediate Robust Protection Following ZIKV Challenge

To assess the kinetics and immune responses that mediate vaccine protection in greater detail, we immunized non-pregnant Balb/c mice with 10^9 vp Ad26.M-Env and challenged them IV with 10^2 PFU ZIKV-BR at week 4 after vaccination (Figure 6A). We utilized immunocompetent Balb/c mice rather than immunodeficient IFN-αβR$^{-/-}$ mice in this experiment to assess wildtype immune responses following ZIKV challenge. No ZIKV RNA was detected in serum from vaccinated mice at 1 hour and on days 1, 2, 4, and 7 following challenge, and in tissues from vaccinated mice on days 2, 4, and 7 following challenge, indicating very early robust protection (Figure 6B, 6C). We also assessed humoral and cellular immune responses by MN50 and ELISPOT assays, respectively, on days 2, 4, and 7 following challenge. At these timepoints, we detected the emergence of primary immune responses in the sham mice, but we did not detect any evidence of anamnestic immune responses in vaccinated mice, suggesting that vaccine-elicited immune responses, rather than virus-induced anamnestic immune responses, were responsible for the immediate and robust protection (Figure 6D, 6E).

Postnatal Protection Against ZIKV Challenge

We finally sought to investigate whether vaccination of dams could afford protection of pups against postnatal ZIKV challenge after birth. Female IFN-αβR$^{-/-}$ mice were vaccinated with 10^9 vp Ad26.M-Env, and six months after immunization, vaccinated mice were mated with wildtype C57BL/6 male mice (Figure 7A). Pregnant mice were allowed to deliver their pups, and ZIKV-specific neutralizing antibodies were observed in the pups (mean MN50 titer 3.06 logs; Figure 7B), with IgG titers higher than IgA titers (Figure 7C, 7D), presumably reflecting passively transferred maternal antibodies. Pups were then challenged IV with 10^2 PFU ZIKV-BR at week 4. Pups born to vaccinated dams demonstrated no detectable serum ZIKV RNA on days 1, 3, and 7 following challenge, whereas pups born to sham control dams exhibited high levels of ZIKV RNA following challenge (Figure 7E). Viremia was controlled by day 7 in the sham group as expected, since they were IFN-αβR$^{-/+}$ heterozygotes. These data demonstrate that Ad26.M-Env vaccination of dams protected their pups against postnatal ZIKV challenge after birth, presumably by passive transfer of maternal antibodies.

DISCUSSION

In this study, we demonstrate that RhAd52.M-Env and Ad26.M-Env vaccines afforded robust protection of pregnant IFN-αβR$^{-/-}$ mice and their fetuses against ZIKV challenge. Maternal antibodies from vaccinated dams also protected pups against ZIKV challenge after birth. These data suggest that vaccine-elicited antibodies can provide robust maternal-fetal

protection as well as postnatal protection, although implications for humans remain to be determined. Moreover, future research will need to explore the impact of cross-reactivity between ZIKV vaccines and other flaviviruses such as dengue.

ZIKV has been shown to induce fetal neuropathology in both mice and monkeys (Martinot et al., 2018; Miner et al., 2016; Uraki et al., 2017; Yockey et al., 2016). While many ZIKV vaccines currently under development have shown the capacity to protect against systemic viremia after challenge, very few have been tested for their ability to prevent fetal infection in pregnant females (Prow et al., 2018; Richner et al., 2017; Wang et al., 2018). In one study, live attenuated virus and RNA-based ZIKV vaccines were tested in pregnant C57BL/6 mice treated with an anti-IFNα receptor antibody prior to ZIKV challenge. Both vaccines provided partial protection and reduced viremia, but virus was still readily detected in multiple maternal and fetal tissues (Richner et al., 2017).

A recent study using a vaccinia-based ZIKV vaccine also reported partial suppression of viremia in pregnant IFN-αβR$^{-/-}$ mice (Prow et al., 2018). Another study reported that a live attenuated virus vaccine reduced viremia in peripheral blood, spleen, and brain tissues in pregnant mice (Xie et al., 2018). Our findings confirm and extend these prior observations in pregnant IFN-αβR$^{-/-}$ mice (Miner et al., 2016; Yockey et al., 2016). We evaluated protective efficacy of Ad26 and RhAd52 vector-based vaccines expressing ZIKV M-Env against IV ZIKV-BR challenge at two doses (10^2 and 10^3 PFU IV). The majority of vaccinated mice showed no ZIKV RNA in maternal and fetal tissues, although a few animals demonstrated low levels of ZIKV RNA, particularly at the higher challenge dose (Figure S3, S4). Moreover, we observed that robust early protection did not involve anamnestic cellular or humoral immune responses in vaccinated mice following ZIKV challenge (Figure 6), suggesting that vaccine-elicited immune responses afforded immediate and effective protection.

It has been reported that newborns can be exposed to ZIKV via breastfeeding (Blohm et al., 2017). During the first year of life, the brain undergoes developmental changes, and ZIKV exposure can lead to complications such as encephalopathy, cognitive impairment, and behavioral alterations (Lavenex et al., 2007). This pathology was also observed in infant nonhuman primates challenged with ZIKV, leading to structural abnormalities in the brain (Mavigner et al., 2018). In a prior study, suckling wild type Balb/c mice born to DNA vaccinated dams were challenged with ZIKV one day after delivery; ZIKV viremia was reduced, but virus could still be detected in peripheral blood and brain tissues (Wang et al., 2018). In the present study, we show that pups born to vaccinated dams were effectively protected against postnatal ZIKV challenge, presumably by passively acquired maternal antibodies.

In summary, our data demonstrate that Ad vector-based vaccines elicited potent ZIKV-specific neutralizing antibodies and robustly protected fetuses in utero and infants after birth against ZIKV challenge. Previous studies in nonhuman primates reported long-term durability of neutralizing antibody responses elicited by Ad-based ZIKV vaccines (Abbink et al., 2017), and clinical trials with these vaccines are currently underway. Taken together,

these findings suggest that Ad vector-based vaccines should be explored further as a strategy to prevent congenital Zika syndrome in humans.

STAR METHODS

LEAD CONTACT AND MATERIALS AVAILABILITY

Further information and requests for resources and reagents should be directed to and will be fulfilled by the Lead Contact, Dr. Dan H. Barouch (dbarouch@bidmc.harvard.edu).

EXPERIMENTAL MODEL AND SUBJECT DETAILS

Experimental Animals—Six weeks old IFNαβR$^{-/-}$ (B6.129S2-*Ifnar1*^{tm1Agt}/Mmjax) female, ten weeks old C57BL/6 male mice, and six-week-old Balb/c female mice were purchased from Jackson Laboratory (Bar Harbor, ME). Four weeks after vaccination, IFNαβR$^{-/-}$ female mice were mated with naïve C57BL/6 male mice in individual cages and after vaginal plug detection, females were grouped in cages. At embryonic day e5.5 after vaginal plug detection, mice were challenged IV with 10^2 or 10^3 PFU ZIKV-BR. Mice were sacrificed at day e9.5 or e17.5 and placentas and fetuses were harvested. Fetal body weight, fetal body length, fetal head size, and fetal body area were measured. For the passive protection study, Ad26.M-Env vaccinated female IFNαβR$^{-/-}$ mice were mated with naïve C57BL/6 male mice six months after vaccination. At week 4 after birth, IFNαβR$^{-/+}$ heterozygote pups were challenged IV with 10^2 PFU of ZIKV-BR. All animals had access to food and water *ad libitum*. All animal studies were approved by the BIDMC Institutional Animal Care and Use Committee (IACUC).

METHOD DETAILS

Vaccination and Challenge—IFNαβR$^{-/-}$ female mice or Balb/c female mice were vaccinated intramuscularly (IM) with 10^9 vp of RhAd52 or Ad26 expressing ZIKV M-Env (prM-Env amino acids 216 to 794 derived from the BeH815744 isolated with the cleavage peptide deleted), and 4 weeks after vaccination mice were challenged intravenously (IV) with 10^2 or 10^3 plaque-forming units (PFU) (10^5 or 10^6 viral RNA copies respectively) ZIKV-BR. For pregnancy studies, IFNαβR$^{-/-}$ female mice were vaccinated IM with 10^9 vp of RhAd52 or Ad26 expressing ZIKV M-Env.

RT-PCR—RT-PCR assays were utilized to monitor viral loads in serum, lymph node, spleen, ovary, brain, placenta, and resorption. RNA was extracted with a QIAcube HT (Qiagen, Germany). Serum samples were extracted using the Qiacube 96 Cador pathogen HT, and tissue samples were lysed in Qiazol, using the Tissuelyser II (Qiagen, Germany), chloroform treated and extracted with the Qiacube 96 RNeasy HT kit. The wildtype ZIKV BeH815744 Cap gene was utilized as a standard. RNA standards were generated using the AmpliCap-Max T7 High Yield Message Maker Kit (Cell Script) and purified with RNA clean and concentrator kit (Zymo Research, CA, USA). RNA quality and concentration were assessed by the BIDMC Molecular Core Facility. Log dilutions of the RNA standard were reverse transcribed and included with each RT-PCR assay. RT-PCR was run on the Quantstudio 6 Flex (Applied Biosystems). Viral loads were calculated as virus particles (VP) per milliliter or VP per microgram of total RNA as measured on the NanoDrop (Thermo

Scientific, Waltham, MA, USA). Assay sensitivity was >100 copies/ml and > 1 copy / μg total RNA.

Anti-ZIKV IgG and IgA ELISA—Mouse ZIKV Env ELISA kits (Alpha Diagnostic International) were used to determine endpoint antibody titers using a modified protocol. 96-well plates coated with ZIKV Env protein were first equilibrated at room temperature with 300 μl of kit working wash buffer for 5 min. 6 μl of mouse serum was added to the top row, and threefold serial dilutions were tested in the remaining rows. Samples were incubated at room temperature for 1 h, and plates washed 4 times. 100 μl of anti-mouse IgG HRP-conjugate working solution was then added to each well and incubated for 30 min at room temperature. For IgA detection, anti-mouse IgA HRP-conjugated antibody was used. Plates were washed 5 times, developed for 15 min at room temperature with 100 μl of 3,3′, 5,5′ tetramehylbenzidine (TMB) substrate, and stopped by the addition of 100 μl of stop solution. Plates were analyzed at 450 nm / 550 nm on a VersaMax microplate reader using Softmax Pro 6.0 software (Molecular Devices). ELISA endpoint titers were defined as the highest reciprocal serum dilution that yielded an absorbance > 2-fold over background values.

Neutralization Assay—A high-throughput ZIKV microneutralization (MN) assay was used for measuring ZIKV-specific neutralizing antibodies, as previously described (Abbink et al., 2016; Larocca et al., 2016). Briefly, serum samples were serially diluted threefold in 96-well microplates, and 100 μl of ZIKV-PR (PRVABC59) containing 100 PFU was added to 100 μl of each serum dilution and incubated at 35 °C for 2 hours. Supernatants were then transferred to microtiter plates containing confluent Vero cell monolayers (World Health Organization, NICSC-011038011038). After incubation for 4 days, cells were fixed with absolute ethanol/methanol for 1 hour at −20 °C and washed three times with PBS. The pan-flavivirus monoclonal antibody 6B6-C1 conjugated to HRP (6B6-C1 was a gift from J. T. Roehrig, U.S. Centers for Disease Control and Prevention) was then added to each well, incubated at 35 °C for 2 hours, and washed with PBS. Plates were washed, developed with TMB for 50 min at room temperature, and stopped with 1:25 phosphoric acid and absorbance was read at 450 nm. For a valid assay, the average absorbance at 450 nm of three noninfected control wells had to be ≤ 0.5, and virus-only control wells had to be ≥ 0.9. Normalized absorbance values were calculated, and the MN50 titer was determined by a log midpoint linear regression model. The MN50 titer was calculated as the reciprocal of the serum dilution that neutralized ≥ 50 % of ZIKV, and seropositivity was defined as a titer ≥ 10, with the maximum measurable titer of 7290. Log10 MN50 titers are reported.

ELISPOT—ZIKV-specific cellular immune responses were assessed by IFN-γ ELISPOT assays using pool of overlapping 15-amino-acid peptides covering the prM, Env, Cap, and NS1 proteins (JPT). 96-well multiscreen plates (Millipore) were coated overnight with 100 μl per well of 10 μg ml−1 anti-mouse IFN-γ (BD Biosciences) in endotoxin-free Dulbecco's PBS (D-PBS). The plates were then washed three times with D-PBS containing 0.25% Tween 20 (D-PBS-Tween), blocked for 2 h with D-PBS containing 5% FBS at 37 °C, washed three times with D-PBS-Tween, rinsed with RPMI 1640 containing 10% FBS to remove the Tween 20, and incubated with 2 μg ml−1 of each peptide and 5 × 105 mouse splenocytes in triplicate in 100 μl reaction mixture volumes. Following 18 h incubation at

37 °C, the plates were washed nine times with PBS-Tween and once with distilled water. The plates were then incubated with 2 μg ml−1 biotinylated anti-mouse IFN-γ (BD Biosciences) for 2 h at room temperature, washed six times with PBS-Tween, and incubated for 2 h with a 1:500 dilution of streptavidin-alkaline phosphatase (Southern Biotechnology Associates). Following five washes with PBS-Tween and one with PBS, the plates were developed with nitroblue tetrazolium-5-bromo-4-chloro-3-indolyl-phosphate chromogen (Pierce), stopped by washing with tap water, air dried, and read using an ELISPOT reader (Cellular Technology Ltd). The numbers of spot-forming cells (SFC) per 10^6 cells were calculated. The medium background levels were typically < 15 SFC per 10^6 cells.

Immunohistochemistry—Tissues were fixed in 10 % neutral buffered formalin for 48 – 72 hours, transferred to 70 % ethanol and submitted for routine embedding and processing for histopathology. Unstained sections were “baked” then deparaffinized with xylene and rehydrated through graded ethanol. Slides were blocked for endogenous peroxidase and alkaline phosphatase (Dual Klearblock, GBI Labs, Cat #E36–18) followed by heat induced epitope retrieval (HIER) in citrate buffer (Vector Labs, Cat # H-3300). For ZIKV staining, sections were incubated overnight at 4°C with Zika virus envelope mouse monoclonal antibody at 1:500 (Biofront, Cat #BF-1176–56). A mouse-on-mouse polymer-based secondary reagent kit (GBI Labs, Cat #D50–18/D50–6) was applied and the signal was visualized utilizing a Permanent Red chromogen (GBI Labs). ZIKV Env, cytokeratin, and vimentin, GBI Labs Triple staining kit was used (Cat #TS309A-6) with ZIKV Env as described, Cytokeratin (Dako, Cat #Z0622 at 1:250), and Vimentin (Abcam, Clone PUR, Cat #92547 at 1:500). All washes were performed utilizing tris-buffered saline with 0.05 % Tween.

QUANTIFICATION AND STATISTICAL ANALYSIS

Analysis of virologic and immunologic data was performed using GraphPad Prism v7.0c (GraphPad Software, CA, USA). Comparisons of groups were performed using unpaired two-tailed nonparametric Mann-Whitney U test. Fetal resorption rates were analyzed by a chi-square test. Data are presented as means ± SEM.

DATA AND CODE AVAILABILITY

This study did not generate codes or datasets

Supplementary Material

Refer to Web version on PubMed Central for supplementary material.

ACKNOWLEDGMENTS

We thank Helen DeCosta, Denise Glass, Laurie Skowronski, Sandy Vertentes, Lindsay Bright and Ernesto Ospina from Animal Research Facility for help with the experiments. We thank Brianna Alimonti, Kittipos Visitsunthorn, Shant Mahrokhian, David Jetton, Rod Bronson and Priya Gandhi for technical support. We acknowledge the support from the National Institute of Health (AI124377, AI128751) and the Ragon Institute of MGH, MIT, and Harvard.

REFERENCES

Abbink P, Larocca RA, La Barrera, De RA, Bricault CA, Moseley ET, Boyd M, Kirilova M, Li Z, Ng'ang'a D, Nanayakkara O, Nityanandam R, Mercado NB, Borducchi EN, Agarwal A, Brinkman AL, Cabral C, Chandrashekar A, Giglio PB, Jetton D, Jimenez J, Lee BC, Mojta S, Molloy K, Shetty M, Neubauer GH, Stephenson KE, Peron JPS, Zanotto P.M. de A., Misamore J, Finneyfrock B, Lewis MG, Alter G, Modjarrad K, Jarman RG, Eckels KH, Michael NL, Thomas SJ, Barouch DH, 2016 Protective efficacy of multiple vaccine platforms against Zika virus challenge in rhesus monkeys. Science 353, 1129–1132. doi:10.1126/science.aah6157 [PubMed: 27492477]

Abbink P, Larocca RA, Visitsunthorn K, Boyd M, La Barrera, De RA, Gromowski GD, Kirilova M, Peterson R, Li Z, Nanayakkara O, Nityanandam R, Mercado NB, Borducchi EN, Chandrashekar A, Jetton D, Mojta S, Gandhi P, LeSuer J, Khatiwada S, Lewis MG, Modjarrad K, Jarman RG, Eckels KH, Thomas SJ, Michael NL, Barouch DH, 2017 Durability and correlates of vaccine protection against Zika virus in rhesus monkeys. Sci Transl Med 9, eaao4163. doi:10.1126/scitranslmed.aao4163 [PubMed: 29237759]

Blohm GM, Lednicky JA, Márquez M, White SK, Loeb JC, Pacheco CA, Nolan DJ, Paisie T, Salemi M, Rodríguez-Morales AJ, Glenn Morris J Jr, Pulliam JRC, Paniz-Mondolfi AE, 2017 Evidence for Mother-to-Child Transmission of Zika Virus Through Breast Milk. Clinical Infectious Diseases 66, 1120–1121. doi:10.1093/cid/cix968

Brasil P, Pereira JP Jr., Moreira ME, Ribeiro Nogueira RM, Damasceno L, Wakimoto M, Rabello RS, Valderramos SG, Halai U-A, Salles TS, Zin AA, Horovitz D, Daltro P, Boechat M, Raja Gabaglia C, Carvalho de Sequeira P, Pilotto JH, Medialdea-Carrera R, Cotrim da Cunha D, Abreu de Carvalho LM, Pone M, Machado Siqueira A, Calvet GA, Rodrigues Baião AE, Neves ES, Nassar de Carvalho PR, Hasue RH, Marschik PB, Einspieler C, Janzen C, Cherry JD, Bispo de Filippis AM, Nielsen-Saines K, 2016 Zika Virus Infection in Pregnant Women in Rio de Janeiro. N Engl J Med 375, 2321–2334. doi:10.1056/NEJMoa1602412 [PubMed: 26943629]

Cugola FR, Fernandes IR, Russo FB, Freitas BC, Dias JLM, Guimarães KP, Benazzato C, Almeida N, Pignatari GC, Romero S, Polonio CM, Cunha I, Freitas CL, Brandão WN, Rossato C, Andrade DG, Faria D. de P., Garcez AT, Buchpigel CA, Braconi CT, Mendes E, Sall AA, Zanotto P.M. de A., Peron JPS, Muotri AR, Beltrão-Braga PCB, 2016 The Brazilian Zika virus strain causes birth defects in experimental models. Nature 534, 267–271. doi:10.1038/nature18296 [PubMed: 27279226]

Krauer F, Riesen M, Reveiz L, Oladapo OT, Martínez-Vega R, Porgo TV, Haefliger A, Broutet NJ, Low N, WHO Zika Causality Working Group, 2017 Zika Virus Infection as a Cause of Congenital Brain Abnormalities and Guillain–Barré Syndrome: Systematic Review. PLoS Med 14, e1002203–27. doi:10.1371/journal.pmed.1002203 [PubMed: 28045901]

Larocca RA, Abbink P, Peron JPS, Zanotto P.M. de A., Iampietro MJ, Badamchi-Zadeh A, Boyd M, Ng'ang'a D, Kirilova M, Nityanandam R, Mercado NB, Li Z, Moseley ET, Bricault CA, Borducchi EN, Giglio PB, Jetton D, Neubauer G, Nkolola JP, Maxfield LF, La Barrera, De RA, Jarman RG, Eckels KH, Michael NL, Thomas SJ, Barouch DH, 2016 Vaccine protection against Zika virus from Brazil. Nature 536, 474–478. doi:10.1038/nature18952 [PubMed: 27355570]

Lavenex P, Banta Lavenex P, Amaral DG, 2007 Postnatal development of the primate hippocampal formation. Dev. Neurosci 29, 179–192. doi:10.1159/000096222 [PubMed: 17148960]

Martinot AJ, Abbink P, Afacan O, Prohl AK, Bronson R, Hecht JL, Borducchi EN, Larocca RA, Peterson RL, Rinaldi W, Ferguson M, Didier PJ, Weiss D, Lewis MG, La Barrera, De RA, Yang E, Warfield SK, Barouch DH, 2018 Fetal Neuropathology in Zika Virus-Infected Pregnant Female Rhesus Monkeys. Cell 1–23. doi:10.1016/j.cell.2018.03.019

Mavigner M, Raper J, Kovacs-Balint Z, Gumber S, O'Neal JT, Bhaumik SK, Zhang X, Habib J, Mattingly C, McDonald CE, Avanzato V, Burke MW, Magnani DM, Bailey VK, Watkins DI, Vanderford TH, Fair D, Earl E, Feczko E, Styner M, Jean SM, Cohen JK, Silvestri G, Johnson RP, O'Connor DH, Wrammert J, Suthar MS, Sanchez MM, Alvarado MC, Chahroudi A, 2018 Postnatal Zika virus infection is associated with persistent abnormalities in brain structure, function, and behavior in infant macaques. Sci Transl Med 10, eaao6975. doi:10.1126/scitranslmed.aao6975 [PubMed: 29618564]

Miner JJ, Bin Cao, Govero J, Smith AM, Fernandez E, Cabrera OH, Garber C, Noll M, Klein RS, Noguchi KK, Mysorekar IU, Diamond MS, 2016 Zika Virus Infection during Pregnancy in Mice Causes Placental Damage and Fetal Demise. Cell 165, 1081–1091. doi:10.1016/j.cell.2016.05.008 [PubMed: 27180225]

Prow NA, Liu L, Nakayama E, Cooper TH, Yan K, Eldi P, Hazlewood JE, Tang B, Le TT, Setoh YX, Khromykh AA, Hobson-Peters J, Diener KR, Howley PM, Hayball JD, Suhrbier A, 2018 A vaccinia-based single vector construct multi-pathogen vaccine protects against both Zika and chikungunya viruses. Nat Commun 9, 1230. doi:10.1038/s41467-018-03662-6 [PubMed: 29581442]

Richner JM, Diamond MS, 2018 ScienceDirect Zika virus vaccines: immune response, current status, and future challenges. Current Opinion in Immunology 53, 130–136. doi:10.1016/j.coi.2018.04.024 [PubMed: 29753210]

Richner JM, Jagger BW, Shan C, Fontes CR, Dowd KA, Cao B, Himansu S, Caine EA, Nunes BTD, Medeiros DBA, Muruato AE, Foreman BM, Luo H, Wang T, Barrett AD, Weaver SC, Vasconcelos PFC, Rossi SL, Ciaramella G, Mysorekar IU, Pierson TC, Shi P-Y, Diamond MS, 2017 Vaccine Mediated Protection Against Zika Virus-Induced Congenital Disease. Cell 170, 273–283.e12. doi:10.1016/j.cell.2017.06.040 [PubMed: 28708997]

Satterfield-Nash A, Kotzky K, Allen J, Bertolli J, Moore CA, Pereira IO, Pessoa A, Melo F, Santelli ACFES, Boyle CA, Peacock G, 2017 Health and Development at Age 19–24 Months of 19 Children Who Were Born with Microcephaly and Laboratory Evidence of Congenital Zika Virus Infection During the 2015 Zika Virus Outbreak - Brazil, 2017. MMWR Morb. Mortal. Wkly. Rep 66, 1347–1351. doi:10.15585/mmwr.mm6649a2 [PubMed: 29240727]

Shan C, Muruato AE, Jagger BW, Richner J, Nunes BTD, Medeiros DBA, Xie X, Nunes JGC, Morabito KM, Kong W-P, Pierson TC, Barrett AD, Weaver SC, Rossi SL, Vasconcelos PFC, Graham BS, Diamond MS, Shi P-Y, 2017 A single-dose live-attenuated vaccine prevents Zika virus pregnancy transmission and testis damage. Nat Commun 8, 676. doi:10.1038/s41467-017-00737-8 [PubMed: 28939807]

Suy A, Sulleiro E, Rodó C, Vázquez É, Bocanegra C, Molina I, Esperalba J, Sánchez-Seco MP, Boix H, Pumarola T, Carreras E, 2016 Prolonged Zika Virus Viremia during Pregnancy. N Engl J Med 375, 2611–2613. doi:10.1056/NEJMc1607580

Uraki R, Jurado KA, Hwang J, Szigeti-Buck K, Horvath TL, Iwasaki A, Fikrig E, 2017 Fetal Growth Restriction Caused by Sexual Transmission of Zika Virus in Mice. The Journal of Infectious Diseases 215, 1720–1724. doi:10.1093/infdis/jix204 [PubMed: 28472297]

Wang R, Liao X, Fan D, Wang L, Song J, Feng K, Li M, Wang P, Chen H, An J, 2018 Maternal immunization with a DNA vaccine candidate elicits specific passive protection against post-natal Zika virus infection in immunocompetent BALB/c mice. Vaccine 1–11. doi:10.1016/j.vaccine.2018.04.051

Xie X, Kum DB, Xia H, Luo H, Shan C, Zou J, Muruato AE, Medeiros DBA, Nunes BTD, Dallmeier K, Rossi SL, Weaver SC, Neyts J, Wang T, Vasconcelos PFC, Shi P-Y, 2018 A Single-Dose Live-Attenuated Zika Virus Vaccine with Controlled Infection Rounds that Protects against Vertical Transmission. Cell Host and Microbe 24, 487–499.e5. doi:10.1016/j.chom.2018.09.008 [PubMed: 30308155]

Yockey LJ, Varela L, Rakib T, Khoury-Hanold W, Fink SL, Stutz B, Szigeti-Buck K, Van den Pol A, Lindenbach BD, Horvath TL, Iwasaki A, 2016 Vaginal Exposure to Zika Virus during Pregnancy Leads to Fetal Brain Infection. Cell 166, 1247–1256.e4. doi:10.1016/j.cell.2016.08.004 [PubMed: 27565347]

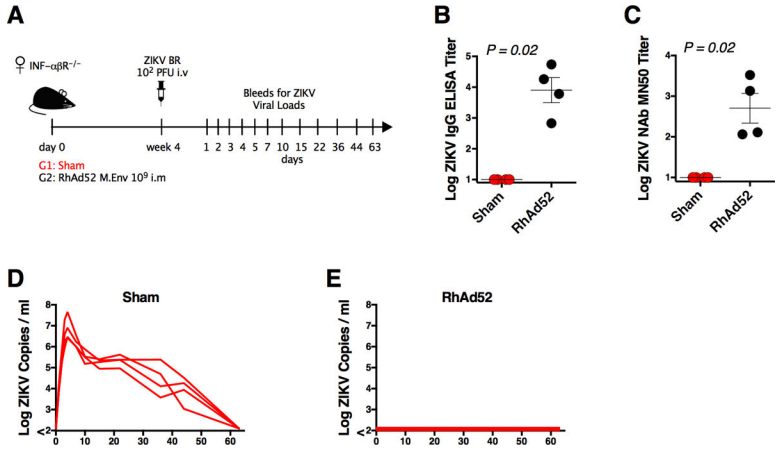

Figure 1. RhAd52 ZIKV Vaccine Protects Non-Pregnant Mice Against ZIKV Challenge.

(A) Study schematic design. IFN-αβR$^{-/-}$ mice were vaccinated IM with 10^9 vp of RhAd52.M-Env (RhAd52) or PBS (Sham) and challenged IV with 10^2 PFU ZIKV-BR 4 weeks after vaccination.

(B) Log ZIKV-specific Env binding antibody titers measured by ELISA in vaccinated versus sham mice at 4 weeks after vaccination.

(C) Log ZIKV-specific microneutralization (MN50) titers in vaccinated versus sham mice at 4 weeks after vaccination.

(D) Log ZIKV viral loads measured by RT-PCR in serum from sham mice.

(E) Log ZIKV viral loads measured by RT-PCR in serum from RhAd52 vaccinated mice.

Data is representative of one experiment with 4 animals per group. Each dot represents an individual mouse. *p* values were calculated using *Mann-Whitney U*. Mean ± SEM is shown. Related to Figure S1.

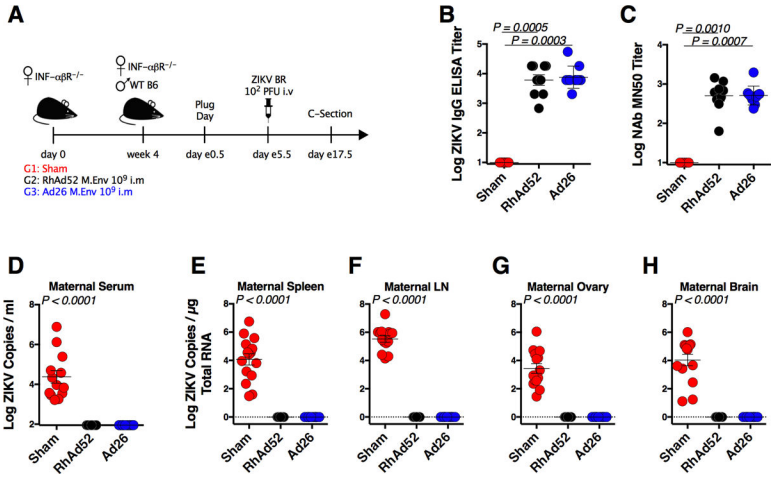

Figure 2. RhAd52 and Ad26 ZIKV Vaccines Protect Pregnant Mice Against ZIKV Challenge.

(A) Study schematic design. IFN-αβR$^{-/-}$ mice were vaccinated IM with 10^9 vp of RhAd52.M-Env (RhAd52), Ad26.M-Env (Ad26), or PBS (Sham). At week 4 after vaccination, IFN-αβR$^{-/-}$ dams were crossed with wildtype males. Pregnant dams were challenged IV with 10^2 PFU ZIKV-BR on day e5.5 followed by harvest of tissues on day e17.5.

(B) Log ZIKV-specific Env binding antibody titers measured by ELISA in vaccinated versus sham mice at 4 weeks after vaccination.

(C) Log ZIKV-specific microneutralization (MN50) titers in vaccinated versus sham mice at 4 weeks after vaccination.

(D-H) Log ZIKV RNA measured by RT-PCR in maternal serum, spleen, lymph node (LN), ovary, and brain.

Data are representative of independent compiled experiments with 9 to 13 animals per group. Each dot represents an individual mouse. *p* values were calculated using *Mann-Whitney U*. Mean ± SEM is shown. The dotted line indicates the limit of detection of the assay.

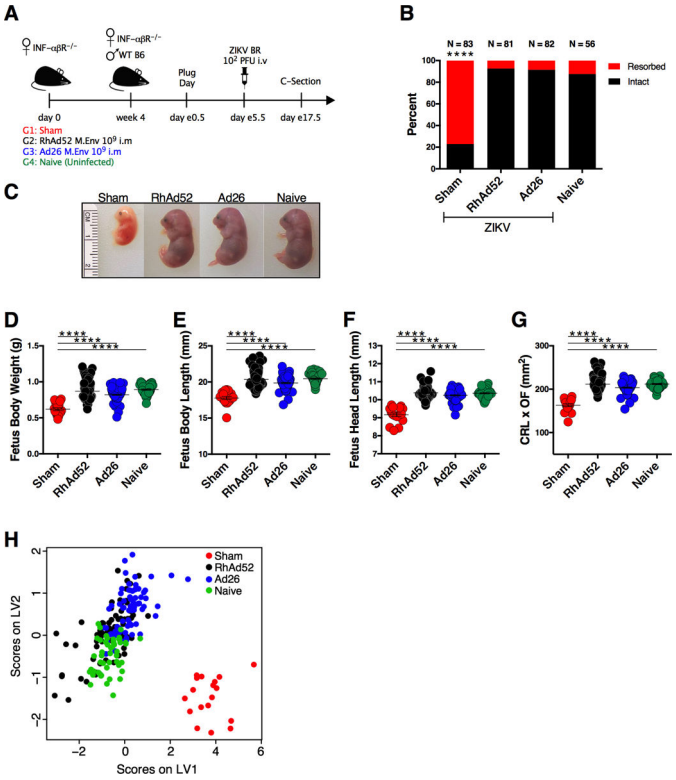

Figure 3. RhAd52 and Ad26 ZIKV Vaccines Prevent Fetal Intrauterine Growth Restriction Following ZIKV Challenge.

(A) Study schematic design. IFN-αβR$^{-/-}$ mice were vaccinated IM with 10^9 vp of RhAd52.M-Env (RhAd52), Ad26.M-Env (Ad26), or PBS (Sham). At week 4 after vaccination, IFN-αβR$^{-/-}$ dams were crossed with wildtype males. Pregnant dams were challenged IV with 10^2 PFU ZIKV-BR on day e5.5 followed by harvest of tissues on day e17.5. Naïve mice were not challenged.

(B) Resorption rate in Sham, RhA52, Ad26, and Naïve groups on day e17.5. Red represents resorbed fetuses, and black represents intact fetuses. The numbers of fetuses for each group are indicated on top of each bar.

(C) Representative fetuses in Sham, RhAd52, Ad26, and Naïve groups.

(D-G) Fetal body weight (grams), body length (mm), head length (mm), and CRL × OF diameter (mm^2). ns (non-significant), *p = 0.021, ***p = 0.0001, ****p < 0.0001.

(H) Partial least squares discriminant analysis of biometric measurements from Sham (red), RhAd52 (black), Ad26 (blue), and Naïve (green) groups.

Data are representative of independent compiled experiments with a total of 56 to 86 animals per group. Each dot represents an individual mouse. *p* values were calculated using *Mann-Whitney U*. Mean ± SEM is shown. Related to Figure S2.

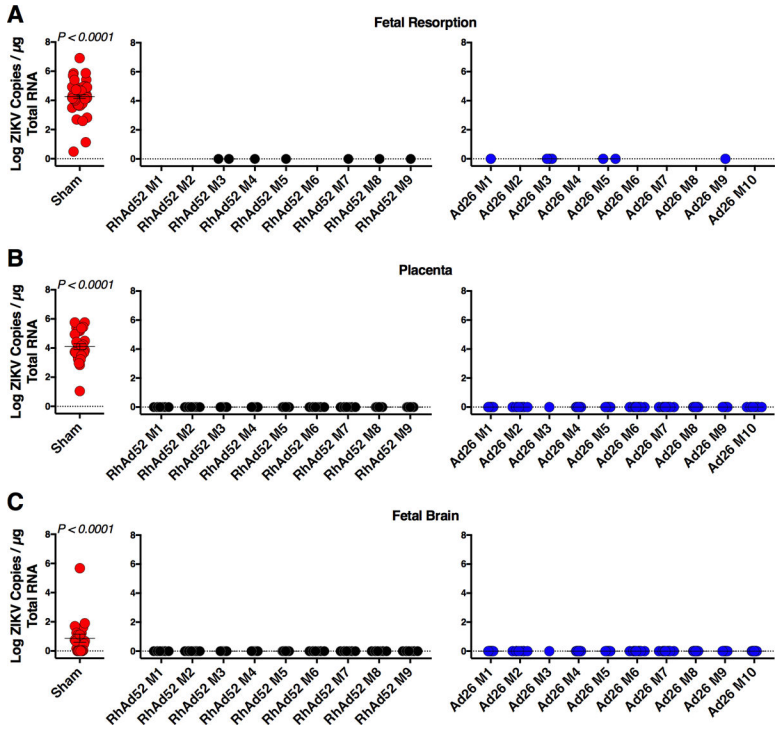

Figure 4. RhAd52 and Ad26 ZIKV Vaccines Protect Placental and Fetal Tissues Following ZIKV Challenge.

(A-C) IFN-αβR$^{-/-}$ mice were vaccinated IM with 10^9 vp of RhAd52.M-Env (RhAd52), Ad26.M-Env (Ad26), or PBS (Sham). At week 4 after vaccination, IFN-αβR$^{-/-}$ dams were crossed with wildtype males. Pregnant dams were challenged IV with 10^2 PFU ZIKV-BR on day e5.5 followed by harvest of tissues on day e17.5. Naïve mice were not challenged.

(A) Log ZIKV viral loads measured by RT-PCR in fetal resorptions.

(B) Log ZIKV viral loads measured by RT-PCR in placenta.

(C) Log ZIKV viral loads measured by RT-PCR in fetal brain.

Data are representative of independent experiments with 56 to 86 animals per group. For vaccinated groups data are plotted for individual dams (M1–M9 (RhAd52) and M1–M10 (Ad26)). Each dot represents an individual mouse. *p* values were calculated using *Mann-Whitney U*. Mean ± SEM is shown. Related to Figures S3, S4.

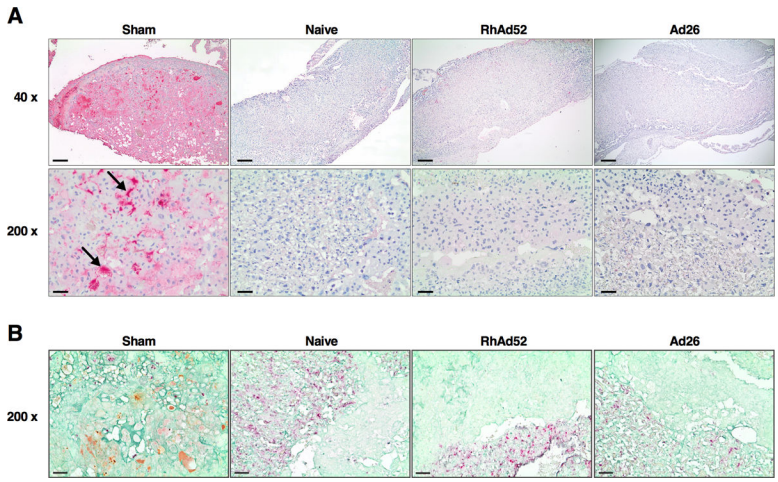

Figure 5. Placenta Immunohistochemistry (IHC) Following ZIKV Challenge.

(A) IHC for ZIKV Env in placenta from Sham, Naïve, RhA52, and Ad26 groups as described in Figure 4. Scale bars, 200 μm (upper), 40 μm (lower).

(B) IHC for ZIKV Env (brown), vimentin (red), and cytokeratin (green) in placenta from Sham, Naïve, RhA52, and Ad26 groups. Scale bars, 200 μm.

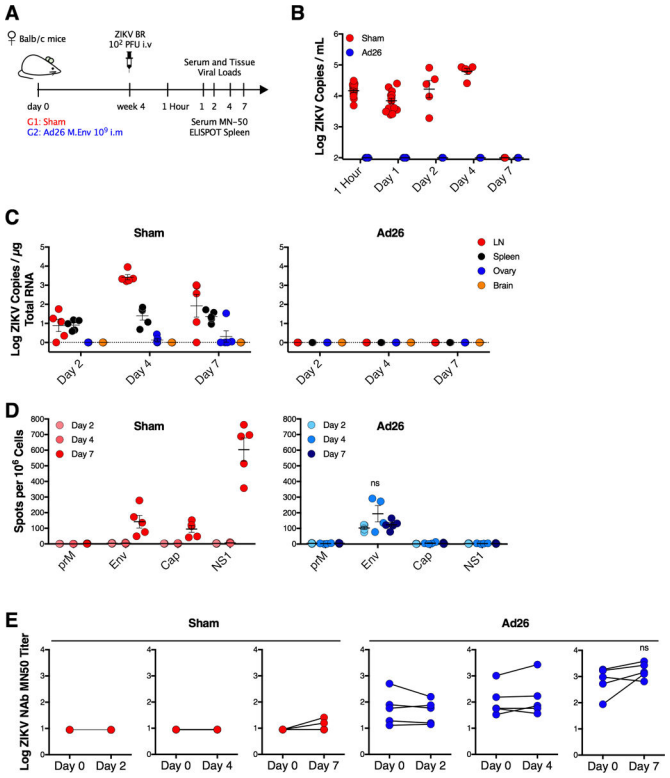

Figure 6. Vaccine-Elicited Immune Responses Mediate Immediate Robust Protection Following ZIKV Challenge.

(A) Study schematic design. Balb/c mice were vaccinated IM with 10^9 vp of Ad26.M-Env (Ad26) or PBS (Sham) and challenged IV with 10^2 PFU ZIKV-BR 4 weeks after vaccination.

(B) Log ZIKV viral loads measured by RT-PCR in serum from sham and Ad26 vaccinated mice.

(C) Log ZIKV RNA measured by RT-PCR in lymph node, spleen, ovary, and brain in sham and Ad26 vaccinated mice.

(D) Interferon-γ ELISPOT assays in response to prM, Env, Cap, and NS1 peptide pools on days 2, 4, and 7 after ZIKV challenge in sham and Ad26 vaccinated mice. Spot-forming cells per 10^6 splenocytes are shown.

(E) Log ZIKV-specific MN50 titers on days 0, 2, 4, and 7 after ZIKV challenge in sham and Ad26 vaccinated mice.

Data is representative of one experiment with 5 animals per group. Each dot represents an individual mouse. *p* values were calculated using *Mann-Whitney U*. Mean ± SEM is shown.

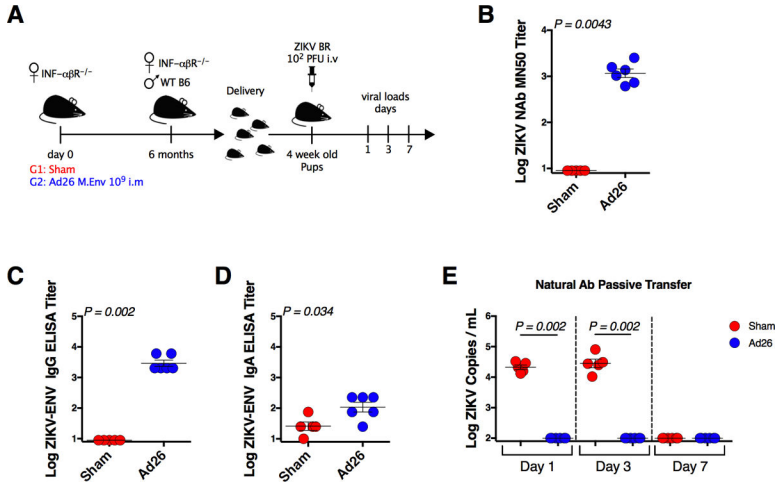

Figure 7. Postnatal Protection Against ZIKV Challenge.

(A) Study schematic design. IFN-αβR$^{-/-}$ mice were vaccinated IM with 10^9 vp of Ad26.M-Env (Ad26) or PBS (Sham). At month 6 after vaccination, IFN-αβR$^{-/-}$ dams were crossed with wildtype males. Pups were challenged IV with 10^2 PFU ZIKV-BR at week 4 after birth.

(B) Log ZIKV-specific MN50 titers in 4 week old pups born to Ad26 or Sham vaccinated dams.

(C) Log ZIKV-specific IgG binding antibody titers in 4 week old pups born to Ad26 or Sham vaccinated dams.

(D) Log ZIKV-specific IgA binding antibody titers in 4 week old pups born to Ad26 or Sham vaccinated dams.

(E) Log ZIKV RNA measured by RT-PCR in serum on day 1, 3, and 7 following challenge.

Key Resources Table

REAGENT or RESOURCE	SOURCE	IDENTIFIER
Antibodies		
Monoclonal Mouse Anti-ZIKV Env	Biofront	Cat# BF-1176-56-100UG; RRID:AB_2687892
Polyclonal Rabbit Anti-Cytokeratin	Dako	Cat# Z0622; RRID:AB_2650434
Vimentin Antibody	Abcam	Cat# ab92547; RRID:AB_10562134
Rat Anti-mouse IFN-γ Monoclonal Antibody	BD Bioscience	Cat# 551216; RRID:AB_394094
Rat Anti-mouse IFN-γ Monoclonal Antibody, Biotinilated	BD Bioscience	Cat# 554410; RRID:AB_395374
Goat Anti-mouse IgA-HRP Antibody	Southern Biothechnology Associates	Cat# 1040-05; RRID:AB_2714213
Rabbit Anti-mouse IgG (H+L) Antibody	Jackson ImmunoResearch Labs	Cat# 315-035-045; RRID:AB_2340066
Bacterial and Virus Strains		
ZIKV-BR; Brazil/ZKV2015, GenBank: KU497555	Cugola et al., 2016	N/A
Biological Samples		
ZIKV Infected Mouse Tissues	This paper	N/A
Uninfected Mouse Tissues	This paper	N/A
Chemicals, Peptides, and Recombinant Proteins		
prM, Env, Cap, and NS1 peptide pools	JPT, Germany Abbink et al., 2016	PepMixes Zika Virus ULTRA
MultiScreen HTS Filter Plate	Millipore	Cat# MSIPS4W10
Streptavidin-alkaline Phosphatase	Southern Biotechnology Associates	Cat # 7100-04
1-Step™ NBT/BCIP Substrate Solution	ThermoFisher Scientific	Cat# 34042
2-Mercaptoethanol (1,000X), Liquid	ThermoFisher Scientific	Cat# 21985023
TWEEN® 20	Millipore-Sigma	Cat# P2287-500mL
Concanavalin A	Millipore-Sigma	Cat# 5275-5mg
MEM Non-Essential Amino Acids Solution	ThermoFisher Scientific	Cat# 11140050
10% Neutral Buffered Formalin	Millipore-Sigma	Cat# HT501128-4L
Xylene	Millipore-Sigma	Cat# 534056
Antigen Unmasking Solution, Citric Acid Based Antibody	Vector Labs	Cat # H-3300; RRID:AB_2336226
Klear Dual Enzyme Block	GBI Labs	Cat# E36-18
Gill's Hematoxylin	VWR	Cat# 100504-388
Eosin	VWR	Cat # 95057-848
Ethanol 190 Proof	VWR	Cat# 700000-282
Tris Buffered Saline, with Tween® 20, pH 7.5	Millipore-Sigma	Cat# SRE0031-500ML
RPMI	Corning	Cat# 10-047-CV
DPBS	ThermoFisher Scientific	Cat# 14190-144
FBS	Millipore-Sigma	Cat# F2442-500ml
Pen/Strep	ThermoFisher Scientific	Cat# 10378016
100x L-glutamine	Lonza	Cat# 17-605E

REAGENT or RESOURCE	SOURCE	IDENTIFIER
QIAzol Lysis Reagent	Qiagen	Cat# 79306
Isoflurane	Patterson Veterinary Supply	Cat# 1169567762
Critical Commercial Assays		
QIAcube HT	Qiagen	Cat# 9001793
Cador Pathogen 96 QIAcube HT Kit	Qiagen	Cat# 54161
RNeasy 96 QIAcube HT Kit	Qiagen	Cat# 74171
RNA Clean & Concentrator™−5	Zymo Research	Cat# R1015
Klear Mouse AP with Fast Red Kit	GBI Labs	Cat# D50-18/D50-6
Polink TS-MRR-Ms A Kit	GBI Labs	Cat# TS309A-6
Mouse anti-ZIKV Env ELISA kit	Alpha Diagnostics	Cat# RV-403120-1
Deposited Data		
Experimental Models: Cell Lines		
Vero Cells	World Health Organization, NICSC-011038011038	N/A
Experimental Models: Organisms/Strains		
Balb/cJ Mouse	The Jackson Laboratory	Cat# 000651
C57BL/6J Mouse	The Jackson Laboratory	Cat# 000664
B6.129S2-Ifnar1tm1Agt/Mmjax (IFN-αβR−/−)	the Jackson Laboratory	Cat# 32045-JAX
Oligonucleotides		
ZIKV.Cap.RT.probe AGTTCAAGAAAGATCTGGCTG	Larocca et al. 2016	N/A
ZIKV.Cap.RT.fwd GGAAAAAAGAGGCTATGGAAATAATAAAG	Larocca et al. 2016	N/A
ZIKV.Cap.RT.rev CTCCTTCCTAGCATTGATTATTCTCA	Larocca et al. 2016	N/A
Zika virus strain BeH815744, GenBank: KU365780	Homo sapiens	N/A
ZIKV Cap mRNA Standards	Larocca et al., 2016	N/A
Recombinant DNA		
Software and Algorithms		
GraphPad Prism v6.03	GraphPad Software	www.graphpad.com/
Softmax Pro 6.0 Software	Molecular Devices	www.moleculardevice.com
Fuji Synapse PACS 3D Software	FujiFILM	www.fujifilm.com
ELISPOT Reader with Immunospot Software	Cellular Technology Ltd	N/A
VersaMax Microplate Reader Using Softmax Pro 6.0 Software	Molecular Devices	Part# VERSAMAX
Other		
Microneutralization (MN) Assay	WRAIR (Larocca et al. 2016)	N/A